A New Finite Volume Scheme for Solving Maxwell System

Malika Remaki

INRIA

INSTITUT NATIONAL DE RECHERCHE EN INFORMATIQUE ET EN AUTOMATIQUE

A New Finite Volume Scheme for Solving Maxwell System

Malika Remaki

N° 3725

1999

THÈME 4

ISSN 0249-6399

A New Finite Volume Scheme for Solving Maxwell System

Malika Remaki

Thème 4 — Simulation et optimisation
de systèmes complexes
Projet CAIMAN

Rapport de recherche n° 3725 — 1999 — 26 pages

Abstract: In this paper, we present a new finite volume scheme to resolve the Maxwell equations. The approach consists of a leapfrog time scheme and a centered flux formula. This method is well suited for handling complex geometries, therefore we use unstructured grids. An analysis of the scheme is presented and numerical experiments are performed.

Key-words: Electromagnetism - Maxwell equations - Finite Volume -Stability.

Unité de recherche INRIA Sophia Antipolis
2004, route des Lucioles, B.P. 93, 06902 Sophia Antipolis Cedex (France)
Téléphone : 04 92 38 77 77 - International : +33 4 92 38 77 77 — Fax : 04 92 38 77 65 - International : +33 4 92 38 77 65

Un nouveau schéma volumes finis pour le système de Maxwell

Résumé : Nous proposons dans ce rapport un schéma volumes finis pour la résolution du système de Maxwell basé sur un schéma Saute-Mouton en temps, et un calcul de flux centrés en espace. Une étude de stabilité du schéma et quelques résultats numériques seront également présentés. L'avantage de ce schéma est son coût relativement faible, et sa capacité à traiter des problèmes avec des géométries quelconques.

Mots-clés : Électromagnétisme - Équations de Maxwell - Volumes Finis - Stabilité.

Contents

1 Introduction

The finite volume methods are considered now as classical techniques to solve conservative laws problems. It derived by integrating the basic equations over a grid cell and construct discrete approximations for the resulting integral terms, which provides a very natural way to use unstructured meshes that conform to complex geometries . F.Hermeline [3], N.K.Madsen and R.W.Ziolkwski [4] proposed methods for the Maxwell equations which require a primary grid and a dual grid based on the Delaunay-Voronoï meshes. These techniques were also used by K.S.Yee ([10], [11]) to construct a hybrid scheme combining a finite difference and a finite volume methods applied to the Maxwell system. The main drawback of these methods is the difficulty to find tridimensional mesh generators. Others types of finite volume methods have also been investigated ([6], [2]), where all the field vectors are located at the same points. These methods use an upwind scheme for the space approximation with a MUSCL technique to get a high order scheme, and a Runge-Kutta sheme for the time discretization. To avoid confusion, we denote these methods a MUSCL finite volume schemes. These methods give a good resolution, but they require a relatively important CPU time compared to finite differences schemes (Yee's scheme for example [9]). We propose here a more simple and economical finite volume method which is based on a centered space scheme and a
leapfrog scheme for the time discretization. This method is second order accurate, and has no numerical dissipation. We present in this paper some theoretical analysis of this finite volume scheme, and we give some numerical experiments and comparisons with a MUSCL finite volume method.

2 Description of the method

We propose in this paper to construct and study a new finite volume scheme for the Maxwell system. We note that all the fields are located at the same points, and are considered as an approximation of a solution on a volume which is called a cell or a control volume. We consider as control volumes, the elements of the mesh (as in the figure 1 for example). because they are well appropriate to treat problems in heterogeneous media, and to take into account the current sheets.

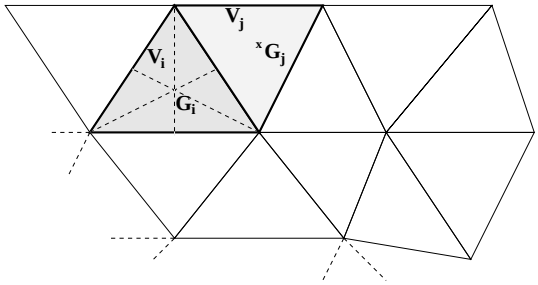

Figure 1: Control volume

2.1 The finite volume scheme

We consider the conservative form of the Maxwell system given by :

$$\frac{\partial \mathbf{Q}}{\partial t} + div\mathbb{F}(\mathbf{Q}) = -\mathbf{J} \tag{1}$$

Where $\mathbf{Q} = {}^t(\mathbf{B}, \mathbf{D})$, $\mathbf{B}$ is the magnetic field and $\mathbf{D}$ is the electric field. $\mathbb{F} = (\mathbf{F_1}, \mathbf{F_2}, \mathbf{F_3})$, with

$$\mathbf{F_1}(\mathbf{Q}) = \begin{Bmatrix} 0 \\ -D_z/\varepsilon \\ D_y/\varepsilon \\ 0 \\ B_z/\mu \\ -B_y/\mu \end{Bmatrix}, \quad \mathbf{F_2}(\mathbf{Q}) = \begin{Bmatrix} D_z/\varepsilon \\ 0 \\ -D_x/\varepsilon \\ -B_z/\mu \\ 0 \\ B_x/\mu \end{Bmatrix}, \quad \mathbf{F_3}(\mathbf{Q}) = \begin{Bmatrix} -D_y/\varepsilon \\ D_x/\varepsilon \\ 0 \\ B_y/\mu \\ -B_x/\mu \\ 0 \end{Bmatrix},$$

Let's consider the elements of the mesh as cells, and integrate the conservative form (1) over each control volume (cell) $\mathbf{V}$.

$$\int_{\mathbf{V}} \frac{\partial \mathbf{Q}}{\partial t}\, dv + \int_{\partial \mathbf{V}} \mathbb{F}(\mathbf{Q}).\mathbf{n}\, ds = 0 \tag{2}$$

Where $\mathbf{n}$ is the outward unit normal to $\mathbf{V}$. Let's suppose that the time derivative is constant on each volume $\mathbf{V}$, then we obtain the following formulation:

$$Volume(\mathbf{V})(\frac{\partial \mathbf{Q}}{\partial t}) + \sum_{\mathbf{V}' \in \mathbf{P}(\mathbf{V})} \mathbf{\Phi}_{\mathbf{V},\mathbf{V}'} = 0 \tag{3}$$

$\mathbf{P}(\mathbf{V})$ denotes the number of neighbours of the volume $\mathbf{V}$, and $\mathbf{\Phi}_{\mathbf{V},\mathbf{V}'}$ a flux function which approach the integral: $\int_{\partial \mathbf{V} \cap \partial \mathbf{V}'} \mathbb{F}(\mathbf{Q}).\mathbf{n}\, ds$.

Flux approximation

We evaluate the flux exchanged between the volume and its neighbours by the following process:

$$\mathbf{\Phi}_{\mathbf{V},\mathbf{V}'} = \widehat{\mathbb{F}}(\mathbf{Q}).\eta = \mathbf{\Phi}(\mathbf{Q}_{\mathbf{V}}, \mathbf{Q}_{\mathbf{V}'})$$

Where $\eta = {}^t(\eta_1, \eta_2) = \int_{\partial \mathbf{V} \cap \partial \mathbf{V}'} \mathbf{n}\, ds$, $\widehat{\mathbb{F}}(\mathbf{Q})$ is an approximation of $\mathbb{F}(\mathbf{Q})$ at the interface $\partial \mathbf{V} \cap \partial \mathbf{V}'$, and $\mathbf{Q}_{\mathbf{V}}$ is the value of the field on the volume $\mathbf{V}$. The centered flux is defined by :

$$\Phi(U, U') = \frac{\mathcal{F}(U, \eta) + \mathcal{F}(U', \eta)}{2}$$

$$\text{With } \mathcal{F}(U, \eta) = \eta.\mathbb{F}(U)$$

Time discretization

After a space discretization, we obtain the following ODE :

$$\frac{d\mathbf{B}}{dt} + \Psi_1(\mathbf{D}) = 0$$

$$\frac{d\mathbf{D}}{dt} + \Psi_2(\mathbf{B}) = 0$$

Where Ψ_1 and Ψ_2 represent the space discretization. For time discretization, we use the second order leapfrog scheme which is defined on each volume by:

$$\begin{cases} \mathbf{B}^{n+\frac{1}{2}} = \mathbf{B}^{n-\frac{1}{2}} - \Delta t \Psi_1(\mathbf{D}^n) \\ \\ \mathbf{D}^{n+1} = \mathbf{D}^n - \Delta t \Psi_2(\mathbf{B}^{n+\frac{1}{2}}) \end{cases} \tag{4}$$

2.2 Analysis of the numerical scheme

We will study in this section, the numerical characteristics of the finite volume scheme described above. We evaluate the scheme order and its domain of stability.

2.2.1 Stability analysis

Proposition 1

For the sake of simplicity, we consider a mesh made up of parallelepipeds (figure2), where the computational domain is unbounded. Thus, the stability of the scheme (4) is ensured by the following criterion:

$$C_{max} \Delta t \sqrt{(\frac{1}{\Delta x^2} + \frac{1}{\Delta y^2} + \frac{1}{\Delta z^2})} \leq 2 \tag{5}$$

Where C_{max} is the maximum wave phase velocity in the computational domain.

Proof of the proposition 1

We consider a normalized region space with $\varepsilon = 1$ and $\mu = 1$, and we denote $(i, j, k) = (i\Delta x, j\Delta y, k\Delta z)$.

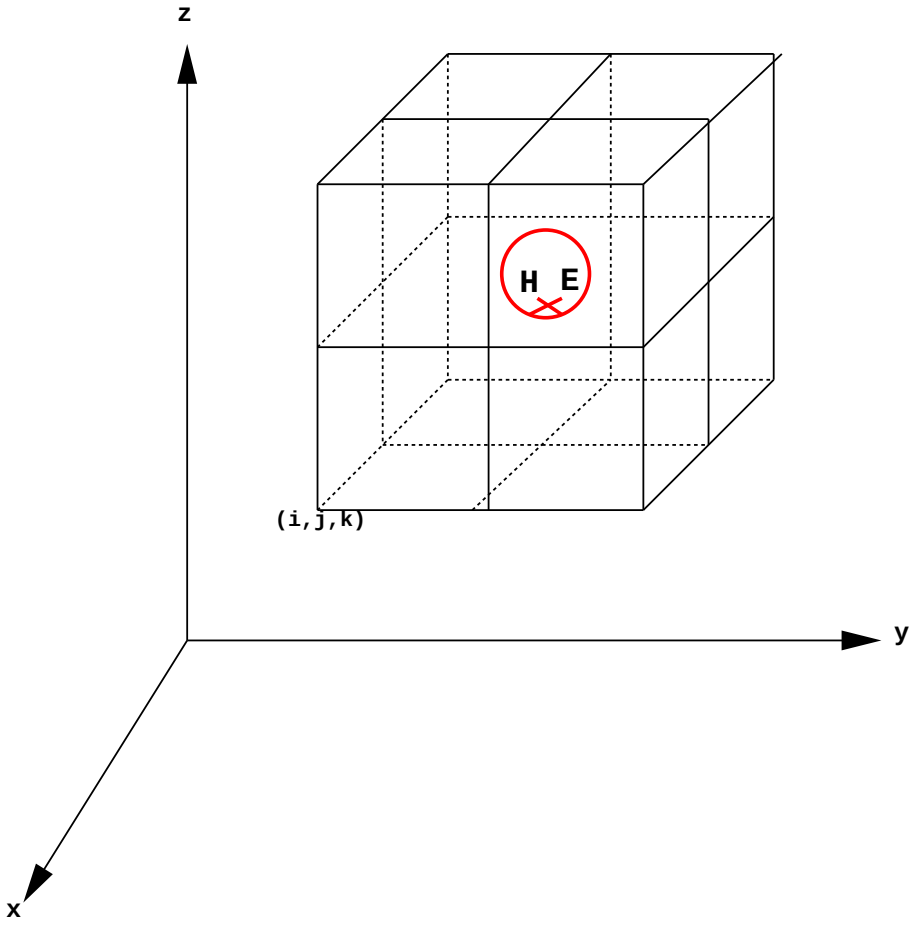

Figure 2: Position of the fields on the finite volume grid

The finite volume scheme is then given by :

$$
\begin{array}{l}
1)\ \mathbf{H}_x^{n+\frac{1}{2}}(i+\frac{1}{2},j+\frac{1}{2},k+\frac{1}{2}) = \mathbf{H}_x^{n-\frac{1}{2}}(i+\frac{1}{2},j+\frac{1}{2},k+\frac{1}{2}) \\
+\frac{\Delta t}{2\Delta z}\left\{\mathbf{E}_y^n(i+\frac{1}{2},j+\frac{1}{2},k+\frac{3}{2}) - \mathbf{E}_y^n(i+\frac{1}{2},j+\frac{1}{2},k-\frac{1}{2})\right\} \\
-\frac{\Delta t}{2\Delta y}\left\{\mathbf{E}_z^n(i+\frac{1}{2},j+\frac{3}{2},k+\frac{1}{2}) - \mathbf{E}_z^n(i+\frac{1}{2},j-\frac{1}{2},k+\frac{1}{2})\right\} \\
\\
2)\ \mathbf{H}_y^{n+\frac{1}{2}}(i+\frac{1}{2},j+\frac{1}{2},k+\frac{1}{2}) = \mathbf{H}_y^{n-\frac{1}{2}}(i+\frac{1}{2},j+\frac{1}{2},k+\frac{1}{2}) \\
+\frac{\Delta t}{2\Delta x}\left\{\mathbf{E}_z^n(i+\frac{3}{2},j+\frac{1}{2},k+\frac{1}{2}) - \mathbf{E}_z^n(i-\frac{1}{2},j+\frac{1}{2},k+\frac{1}{2})\right\} \\
-\frac{\Delta t}{2\Delta z}\left\{\mathbf{E}_x^n(i+\frac{1}{2},j+\frac{1}{2},k+\frac{3}{2}) - \mathbf{E}_x^n(i+\frac{1}{2},j+\frac{1}{2},k-\frac{1}{2})\right\} \\
\\
3)\ \mathbf{H}_z^{n+\frac{1}{2}}(i+\frac{1}{2},j+\frac{1}{2},k+\frac{1}{2}) = \mathbf{H}_z^{n-\frac{1}{2}}(i+\frac{1}{2},j+\frac{1}{2},k+\frac{1}{2}) \\
+\frac{\Delta t}{2\Delta y}\left\{\mathbf{E}_x^n(i+\frac{1}{2},j+\frac{3}{2},k+\frac{1}{2}) - \mathbf{E}_x^n(i+\frac{1}{2},j-\frac{1}{2},k+\frac{1}{2})\right\} \\
-\frac{\Delta t}{2\Delta x}\left\{\mathbf{E}_y^n(i+\frac{3}{2},j+\frac{1}{2},k+\frac{1}{2}) - \mathbf{E}_y^n(i-\frac{1}{2},j+\frac{1}{2},k+\frac{1}{2})\right\} \\
\\
4)\ \mathbf{E}_x^n(i+\frac{1}{2},j+\frac{1}{2},k+\frac{1}{2}) = \mathbf{E}_x^{n-1}(i+\frac{1}{2},j+\frac{1}{2},k+\frac{1}{2}) \\
+\frac{\Delta t}{2\Delta y}\left\{\mathbf{H}_z^{n-\frac{1}{2}}(i+\frac{1}{2},j+\frac{3}{2},k+\frac{1}{2}) - \mathbf{H}_z^{n-\frac{1}{2}}(i+\frac{1}{2},j-\frac{1}{2},k+\frac{1}{2})\right\} \\
-\frac{\Delta t}{2\Delta z}\left\{\mathbf{H}_y^{n-\frac{1}{2}}(i+\frac{1}{2},j+\frac{1}{2},k+\frac{3}{2}) - \mathbf{H}_y^{n-\frac{1}{2}}(i+\frac{1}{2},j+\frac{1}{2},k-\frac{1}{2})\right\} \\
\\
5)\ \mathbf{E}_y^n(i+\frac{1}{2},j+\frac{1}{2},k+\frac{1}{2}) = \mathbf{E}_y^{n-1}(i+\frac{1}{2},j+\frac{1}{2},k+\frac{1}{2}) \\
+\frac{\Delta t}{2\Delta z}\left\{\mathbf{H}_x^{n-\frac{1}{2}}(i+\frac{1}{2},j+\frac{1}{2},k+\frac{3}{2}) - \mathbf{H}_x^{n-\frac{1}{2}}(i+\frac{1}{2},j+\frac{1}{2},k-\frac{1}{2})\right\} \\
-\frac{\Delta t}{2\Delta x}\left\{\mathbf{H}_x^{n-\frac{1}{2}}(i+\frac{3}{2},j+\frac{1}{2},k+\frac{1}{2}) - \mathbf{H}_x^{n-\frac{1}{2}}(i-\frac{1}{2},j+\frac{1}{2},k+\frac{1}{2})\right\} \\
\\
6)\ \mathbf{E}_z^n(i+\frac{1}{2},j+\frac{1}{2},k+\frac{1}{2}) = \mathbf{E}_z^{n-1}(i+\frac{1}{2},j+\frac{1}{2},k+\frac{1}{2}) \\
+\frac{\Delta t}{2\Delta x}\left\{\mathbf{H}_y^{n-\frac{1}{2}}(i+\frac{3}{2},j+\frac{1}{2},k+\frac{1}{2}) - \mathbf{H}_y^{n-\frac{1}{2}}(i-\frac{1}{2},j+\frac{1}{2},k+\frac{1}{2})\right\} \\
-\frac{\Delta t}{2\Delta y}\left\{\mathbf{H}_x^{n-\frac{1}{2}}(i+\frac{1}{2},j+\frac{3}{2},k+\frac{1}{2}) - \mathbf{H}_x^{n-\frac{1}{2}}(i+\frac{1}{2},j-\frac{1}{2},k+\frac{1}{2})\right\}
\end{array}
\tag{6}
$$

We denote :

$$\mathbf{Q}^n_{l,j,k} = \begin{pmatrix} \mathbf{H}_x^{n-\frac{1}{2}}(l+\frac{1}{2}, j+\frac{1}{2}, k+\frac{1}{2}) \\ \mathbf{H}_y^{n-\frac{1}{2}}(l+\frac{1}{2}, j+\frac{1}{2}, k+\frac{1}{2}) \\ \mathbf{H}_z^{n-\frac{1}{2}}(l+\frac{1}{2}, j+\frac{1}{2}, k+\frac{1}{2}) \\ \mathbf{E}_x^{n-1}(l+\frac{1}{2}, j+\frac{1}{2}, k+\frac{1}{2}) \\ \mathbf{E}_y^{n-1}(l+\frac{1}{2}, j+\frac{1}{2}, k+\frac{1}{2}) \\ \mathbf{E}_z^{n-1}(l+\frac{1}{2}, j+\frac{1}{2}, k+\frac{1}{2}) \end{pmatrix}$$

Using the Fourier transformation, yields the following system :

$$\hat{\mathbf{Q}}^{n+1} = \mathbf{G}_{\theta_1,\theta_2,\theta_3}\hat{\mathbf{Q}}^n \tag{7}$$

Where $\theta_1, \theta_2, \theta_3 \in [0, 2\pi]^3$ are the Fourier angles . The amplification matrix $\mathbf{G}_{\theta_1,\theta_2,\theta_3}$ writes in this case :

$$\mathbf{G}_{\theta_1,\theta_2,\theta_3} = Id + \begin{pmatrix} Y_1 & Y_2 & Y_3 & 0 & Y_5 & Y_6 \\ Y_2 & X_2 & X_3 & -Y_5 & 0 & X_6 \\ Y_3 & X_3 & C_3 & -Y_6 & -X_6 & 0 \\ 0 & -Y5 & -Y_6 & 0 & 0 & 0 \\ Y_5 & 0 & X_6 & 0 & 0 & 0 \\ Y_5 & 0 & -X_6 & 0 & 0 & 0 \\ Y_6 & X_6 & 0 & 0 & 0 & 0 \end{pmatrix} \tag{8}$$

Where

$$Y_1 = -\frac{\Delta t^2}{\Delta y^2} sin^2\theta_2 - \frac{\Delta t^2}{\Delta z^2} sin^2\theta_3$$

$$Y_2 = \frac{\Delta t^2}{\Delta x \Delta y} sin\theta_1 sin\theta_2$$

$$Y_3 = \frac{\Delta t^2}{\Delta x \Delta z} sin\theta_1 sin\theta_3$$

$$Y_5 = i\frac{\Delta t}{\Delta z} sin\theta_3$$

$$Y_6 = i\frac{\Delta t}{\Delta y} sin\theta_2$$

$$X_2 = -\frac{\Delta t^2}{\Delta x^2} sin^2\theta_1 - \frac{\Delta t^2}{\Delta z^2} sin^2\theta_3$$

$$X_3 = \frac{\Delta t^2}{\Delta y \Delta z} sin\theta_2 sin\theta_3$$

$$X_6 = i\frac{\Delta t}{\Delta x} sin\theta_1$$

$$C_3 = -\frac{\Delta t^2}{\Delta x^2} sin^2\theta_1 - \frac{\Delta t^2}{\Delta y^2} sin^2\theta_2$$

The necessary and sufficient stability condition (Von Neumann condition) writes:

$$\forall(\theta_1, \theta_2, \theta_3) \in [0, 2\pi], \quad \max_{s=1,2,3,4,5,6} |\lambda^s_{\theta_1,\theta_2,\theta_3}| \leq 1$$

Where the values $\lambda^s_{\theta_1,\theta_2,\theta_3}$ represent the eigenvalues of the amplification matrix. We first consider the eigenvalues of the matrix $\mathbf{H} = \mathbf{G}_{\theta_1,\theta_2,\theta_3} - Id$:

$$det(\mathbf{H} - \lambda Id) = \lambda^2 \left(\lambda^4 + 2\alpha\lambda^3 + (2\alpha + \alpha^2)\lambda^2 + 2\alpha^2\lambda + \alpha^2\right)$$

With

$$\alpha = \frac{\Delta t^2}{\Delta x^2} sin^2\theta_1 + \frac{\Delta t^2}{\Delta y^2} sin^2\theta_2 + \frac{\Delta t^3}{\Delta z^2} sin^2\theta_3$$

Let

$$g(\lambda) = \lambda^4 + 2\alpha * \lambda^3 + (2\alpha + \alpha^2)\lambda^2 + 2\alpha^2\lambda + \alpha^2$$

$$g(\lambda) = (\lambda^2 + \alpha\lambda + \alpha)^2$$

$$g(\lambda) = 0 \Longleftrightarrow \lambda^2 + \alpha\lambda + \alpha = 0$$

The sufficient condition

We have stability of the scheme when $\alpha \leq 4$. We give here the proof : for $\alpha \leq 4$, the eigenvalues $\lambda_{1,2}$ of the matrix $\mathbf{H}$ are given by:

$$\lambda_{1,2} = \frac{-\alpha \pm i\sqrt{4\alpha - \alpha^2}}{2}$$

$$\Longrightarrow \max_i |1 + \lambda_i| = \sqrt{\frac{(2-\alpha)^2 + (4\alpha - \alpha^2)}{4}} = 1$$

Which implies that the scheme is stable.

The necessary condition

We prove here that for $\alpha > 4$, the scheme is instable.
For $\alpha > 4$, we have

$$\lambda_{1,2} = \frac{-\alpha \pm \sqrt{\alpha^2 - 4\alpha}}{2}$$

Suppose that:

$$|1 + \lambda_i| \leq 1$$
$$\Longrightarrow \alpha + \sqrt{\alpha^2 - 4\alpha} \leq 4$$

which is absurd since $\alpha > 4$, therefore the scheme is instable. We deduce from this study the following stability condition :

$$\Delta t \sqrt{(\frac{1}{\Delta x^2} sin^2\theta_1 + \frac{1}{\Delta y^2} sin^2\theta_2 + \frac{1}{\Delta z^2} sin^2\theta_3)} \leq 2 \ \ \forall (\theta_1, \theta_2, \theta_3) \in [0 : 2\pi]^3$$

This stability criterion is true in particular for $\theta_1 = \frac{\pi}{2}$, $\theta_2 = \frac{\pi}{2}$, and $\theta_3 = \frac{\pi}{2}$, which implies the CFL condition (5).

2.2.2 Study of the space accuracy

Proposition 2

The scheme (4) is second order accurate on structured grids.

Description of the modified equation

The modified equation method which was intruduced by Warming and Hyett [8] is a suited technique for the analysis of the order of a numerical method to resolve a linear temporel problems. This method allows to derive the truncature errors. We first recall briefly the basic rules of this method (For more details see [1]). Let's consider a linear evolution partial differential equation in the monodimensional case:

$$u_t = \sum_{k \geq 0} \gamma_k \frac{\partial^k u}{\partial x^k} \tag{9}$$

We approach the equation (9) by an explicit first-order upwind scheme:

$$\frac{u_j^{n+1} - u_j^n}{\Delta t} = \sum_k c_k \, u_{j+k}^n$$

Let $g_{\Delta x}$ the amplification coefficient defined by:

$$g_{\Delta x} = \sum_k c_k \, e^{k \Delta x X}$$

Thus, the modified equation of the above scheme writes:

$$u_t = \sum_{k \geq 0} \alpha_k \frac{\partial^k u}{\partial x^k}$$

Where :

$$\sum_{k \geq 0} \alpha_k \frac{\partial^k u}{\partial x^k}$$

is the formal series expansion of the function:

$$\frac{log(1 + \Delta t g_{\Delta x}(\frac{\partial^k u}{\partial x^k}))}{\Delta t}$$

Proof of the proposition 2

For the sake of simplicity, we will restrict our investigation to the one dimensional case. We propose to prove the above proposition using the modified equation technique. We recall here the finite volume scheme in the normalized case ($\varepsilon = 1$ and $\mu = 1$):

$$\begin{cases} \dfrac{\mathbf{H}_{j+\frac{1}{2}}^{n+\frac{1}{2}} - \mathbf{H}_{j+\frac{1}{2}}^{n-\frac{1}{2}}}{\Delta t} = -\dfrac{1}{2\Delta y} \left(\mathbf{E}_{j+\frac{3}{2}}^n - \mathbf{E}_{j-\frac{1}{2}}^n \right) \\ \dfrac{\mathbf{E}_{j+\frac{1}{2}}^{n+1} - \mathbf{E}_{j+\frac{1}{2}}^n}{\Delta t} = -\dfrac{1}{2\Delta y} \left(\mathbf{H}_{j+\frac{3}{2}}^{n+\frac{1}{2}} - \mathbf{H}_{j-\frac{1}{2}}^{n+\frac{1}{2}} \right) \end{cases} \tag{10}$$

To obtain all the variables at the same time, we use the Taylor series expansion:

$$\mathbf{H}^{n+\frac{1}{2}} = \mathbf{H}^n + \frac{\Delta t}{2}\frac{\partial}{\partial t}\mathbf{H}^n + \frac{\Delta t^2}{8}\frac{\partial^2}{\partial t^2}\mathbf{H}^n + O(\Delta t^3)$$

$$\mathbf{H}^{n-\frac{1}{2}} = \mathbf{H}^n - \frac{\Delta t}{2}\frac{\partial}{\partial t}\mathbf{H}^n + \frac{\Delta t^2}{8}\frac{\partial^2}{\partial t^2}\mathbf{H}^n + O(\Delta t^3)$$

$$\mathbf{E}^n = \mathbf{E}^{n-\frac{1}{2}} + \frac{\Delta t}{2}\frac{\partial}{\partial t}\mathbf{E}^{n-\frac{1}{2}} + \frac{\Delta t^2}{8}\frac{\partial^2}{\partial t^2}\mathbf{E}^{n-\frac{1}{2}} + O(\Delta t^3)$$

$$\mathbf{E}^{n-1} = \mathbf{E}^{n-\frac{1}{2}} - \frac{\Delta t}{2}\frac{\partial}{\partial t}\mathbf{E}^{n-\frac{1}{2}} + \frac{\Delta t^2}{8}\frac{\partial^2}{\partial t^2}\mathbf{E}^{n-\frac{1}{2}} + O(\Delta t^3)$$

Using the modified equation technique and the above development, we get the following modified equation:

$$\begin{cases} \dfrac{\partial}{\partial t}\mathbf{H} = -\dfrac{\partial}{\partial y}\mathbf{E} + O(\Delta t \Delta y) + O(\Delta t^2) + O(\Delta y^2) \\ \dfrac{\partial}{\partial t}\mathbf{E} = -\dfrac{\partial}{\partial y}\mathbf{H} + O(\Delta t \Delta y) + O(\Delta t^2) + O(\Delta y^2) \end{cases}$$

which prove that the scheme (10) is second order accurate in space and time.

2.2.3 Conservation of the numerical energy

We define the discrete energy by:

$$2\mathcal{E}_h = \sum_j (\mathbf{E}^n_{j+\frac{1}{2}})^2 + \mathbf{H}^{n+\frac{1}{2}}_{j+\frac{1}{2}} \times \mathbf{H}^{n-\frac{1}{2}}_{j+\frac{1}{2}} \tag{11}$$

Remark

The formulation (11) is a quadratic and definite positive form for $\nu = \dfrac{\Delta t}{\Delta y} \leq 2$.

Proof

$$2\mathcal{E}_h = \sum_j (\mathbf{E}^n_{j+\frac{1}{2}})^2 + \left(\mathbf{H}^{n-\frac{1}{2}}_{j+\frac{1}{2}} - \frac{\nu}{4}(\mathbf{E}^n_{j+\frac{3}{2}} - \mathbf{E}^n_{j-\frac{1}{2}})\right)^2 - \frac{\nu^2}{16}(\mathbf{E}^n_{j+\frac{3}{2}} - \mathbf{E}^n_{j-\frac{1}{2}})^2$$

We deduce that:

$$2\mathcal{E}_h \geq \sum_j \left(\mathbf{H}^{n-\frac{1}{2}}_{j+\frac{1}{2}} - \frac{\nu}{4}(\mathbf{E}^n_{j+\frac{3}{2}} - \mathbf{E}^n_{j-\frac{1}{2}})\right)^2 + (1 - \frac{\nu^2}{4})(\mathbf{E}^n_{j+\frac{1}{2}})^2$$

$\Longrightarrow 2\mathcal{E}_h \geq 0$ for $\nu \leq 2$.
We also have; $(2\mathcal{E}_h = 0 \Longrightarrow \mathbf{E}_{j+\frac{1}{2}} = 0$ and $\mathbf{H}_{j+\frac{1}{2}} = 0,\ \forall j)$.
The variation of the energy is given by:

$$\begin{aligned}
2\Delta\mathcal{E}_h &= \sum_j ((\mathbf{E}^{n+1}_{j+\frac{1}{2}})^2 - (\mathbf{E}^n_{j+\frac{1}{2}})^2) + (\mathbf{H}^{n+\frac{3}{2}}_{j+\frac{1}{2}} \times \mathbf{H}^{n+\frac{1}{2}}_{j+\frac{1}{2}} - \mathbf{H}^{n+\frac{1}{2}}_{j+\frac{1}{2}} \times \mathbf{H}^{n-\frac{1}{2}}_{j+\frac{1}{2}}) \\
&= \sum_j \frac{\nu^2}{4}(\mathbf{H}^{n+\frac{1}{2}}_{j+\frac{3}{2}} - \mathbf{H}^{n+\frac{1}{2}}_{j-\frac{1}{2}})^2 - \nu\mathbf{E}^n_{j+\frac{1}{2}}(\mathbf{H}^{n+\frac{1}{2}}_{j+\frac{3}{2}} - \mathbf{H}^{n+\frac{1}{2}}_{j-\frac{1}{2}}) - \frac{\nu}{2}\mathbf{H}^{n+\frac{1}{2}}_{j+\frac{1}{2}}(\mathbf{E}^{n+1}_{j+\frac{3}{2}} - \mathbf{E}^{n+1}_{j-\frac{1}{2}}) \\
&\qquad -\frac{\nu}{2}\mathbf{H}^{n+\frac{1}{2}}_{j+\frac{1}{2}}(\mathbf{E}^n_{j+\frac{3}{2}} - \mathbf{E}^n_{j-\frac{1}{2}}) \\
&= \sum_j \frac{\nu^2}{4}(\mathbf{H}^{n+\frac{1}{2}}_{j+\frac{3}{2}} - \mathbf{H}^{n+\frac{1}{2}}_{j-\frac{1}{2}})^2 - \nu\mathbf{E}^n_{j+\frac{1}{2}}(\mathbf{H}^{n+\frac{1}{2}}_{j+\frac{3}{2}} - \mathbf{H}^{n+\frac{1}{2}}_{j-\frac{1}{2}}) - \nu\mathbf{H}^{n+\frac{1}{2}}_{j+\frac{1}{2}}(\mathbf{E}^{n+1}_{j+\frac{3}{2}} - \mathbf{E}^{n+1}_{j-\frac{1}{2}}) \\
&\qquad +\frac{\nu^2}{4}\mathbf{H}^{n+\frac{1}{2}}_{j+\frac{1}{2}}(\mathbf{H}^{n+\frac{1}{2}}_{j+\frac{5}{2}} - 2\mathbf{H}^{n+\frac{1}{2}}_{j+\frac{1}{2}} + \mathbf{H}^{n+\frac{1}{2}}_{j-\frac{3}{2}}) \quad = 0
\end{aligned} \tag{12}$$

Which implies the conservation of the discrete energy.

2.2.4 Study of the numerical dispersion

We propose here to evaluate the degree of the dispersion of the scheme. First, we recall the dispersion relation in the continuous case, it's given by:

$$\omega^2 = |k|^2 C^2 \tag{13}$$

This relation is verified by non dissipative waves with wave phase velocity $\pm C$. We deduce the discrete wave equation from the finite volume scheme:

$$\begin{array}{l}\frac{E^{n+1}(i,j,k)-2E^n(i,j,k)+E^{n-1}(i,j,k)}{\Delta t^2} = C^2\left(\frac{E^n(i+2,j,k)+E^n(i-2,j,k)-2E^n(i,j,k)}{4\Delta x^2}\right) \\ +C^2\left(\frac{E^n(i,j+2,k)+E^n(i,j-2,k)-2E^n(i,j,k)}{4\Delta y^2} + \frac{E^n(i,j,k+2)+E^n(i,j,k-2)-2E^n(i,j,k)}{4\Delta z^2}\right)\end{array} \tag{14}$$

we consider the harmonic wave:

$$E(j\Delta x, l\Delta y, m\Delta z, n\Delta t) = E_0 e^{i[\omega n\Delta t-(k_x j\Delta x+k_y l\Delta y+k_z m\Delta z)]}$$

Injecting this expression in (14), yields:

$$sin^2\frac{\omega\Delta t}{2\Delta t^2} = \frac{C^2}{4}\left(\frac{sin^2 k_x\Delta x}{\Delta x^2} + \frac{sin^2 k_y\Delta y}{\Delta y^2} + \frac{sin^2 k_z\Delta z}{\Delta z^2}\right) \tag{15}$$

It represents the numerical dispersion relation. The Taylor series expansion of (15) gives:

$$\omega^2(1+O(\omega^2\Delta t^2)) = C^2|k|^2(1+O(\frac{k_x^4\Delta x^2+k_y^4\Delta y^2+k_z^4\Delta z^2}{|k|^2})) \tag{16}$$

Where

$$|k|^2 = k_x^2+k_y^2+k_z^2$$

The relationship (16) shows that the numerical method presents a second order dispersive error. We compare now this error to the dispersive error given by Yee's scheme [9]. Using the Taylor series expansion, the dispersive relationship given by both methods (Yee's method and the finite volume method) writes:

The finite volume dispersion

$$\begin{array}{l}\omega^2(1-\frac{\omega^2\Delta t^2}{12}+O(\omega^4\Delta t^4)) = \\ C^2|k|^2\left(1-\frac{1}{3}(\frac{k_x^4\Delta x^2+k_y^4\Delta y^2+k_z^4\Delta z^2}{|k|^2})+O(\frac{k_x^6\Delta x^4+k_y^6\Delta y^4+k_z^6\Delta z^4}{|k|^2})\right)\end{array} \tag{17}$$

The Yee's scheme dispersion

$$\omega^2(1-\frac{\omega^2\Delta t^2}{12}+O(\omega^4\Delta t^4))=$$

$$C^2|k|^2\left(1-\frac{1}{12}(\frac{k_x^4\Delta x^2+k_y^4\Delta y^2+k_z^4\Delta z^2}{|k|^2})+O(\frac{k_x^6\Delta x^4+k_y^6\Delta y^4+k_z^6\Delta z^4}{|k|^2})\right) \tag{18}$$

Assume that

$$\Delta t \leq \frac{\sqrt{3}}{\pi}\times T \quad \text{with} \quad T=\frac{2\pi}{\omega} \quad \text{is a period.}$$

Then, we can deduce that both schemes present a second order dispersive error, however the Yee's scheme has little less numerical dispersion than the finite volume one. Therefore it will be interesting to construct a hybrid scheme combining both methods in order to exploit the different advantages, which are the ability of the finite volume scheme to treat complex geometries, and the smaller amount of a numerical dispersion of the Yee's scheme in the structured grids. We can notice that both methods are economical and simple to implement.

3 Numerical experiments

We give here some numerical experiments in order to validate the finite volume method described above. The meshes used are unstructured ones. The first test consists in computing the evolution of a mode of resonance in a cavity. We also give an example of an electromagnetic field produced by a sheet of current over a cross section of a rectangular waveguide. Another test consists in a qualitative analysis in an heterogeneous case. It represents a propagation of a pulse into a material composed of a vacuum and a glass. Lastly, we simulate the scattered wave across a dielectrical material.

3.1 Evolution of a mode of resonance

We give here the evolution of a mode of resonance in a metallic cavity. The number of points per wavelenght is arround 12. We first compare the numer-

ical solution to the exact one (figure 3 is a zoom of the numerical solution). We can notice that we have a good resolution for 70 wavelenghts, and the numerical solution is not dispersive, neither diffusive. The (figure 4) shows the conservation of the numerical energy. This is matches to the theoretical results given in the begining of this study.

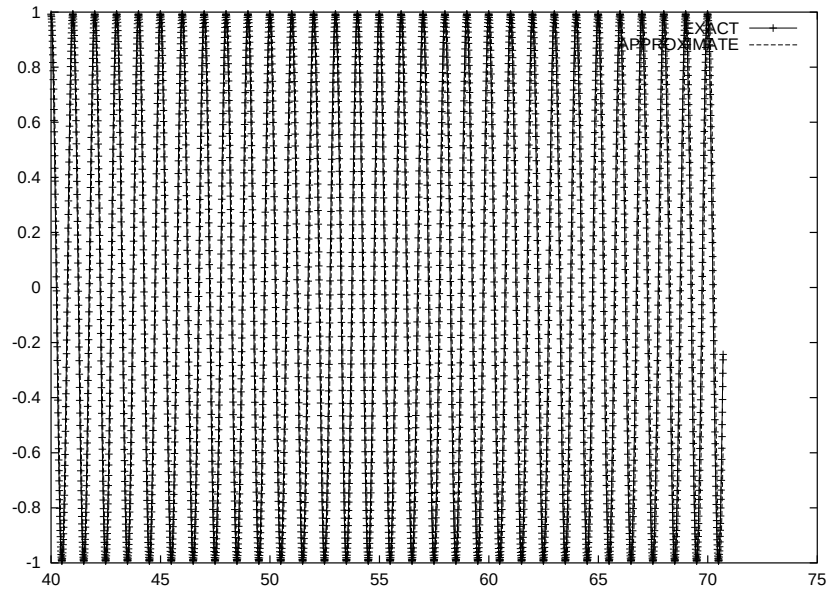

Figure 3: Time evolution of a mode of resonance between 40 and 70 wavelenghts

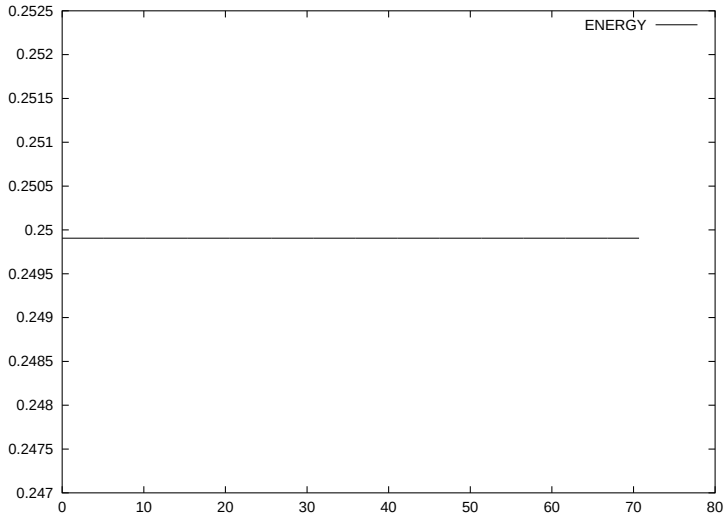

Figure 4: Discrete energy

3.2 The rectangular waveguide

Consider a currrent $\mathbf{J}_s$ over the cross section of a rectangular waveguide on $x = 0$ (figure 5) given by:

$$J_s = \sqrt{2} sin(\frac{\pi y}{d}) cos(\omega t) \tag{19}$$

In this experiment, we fixed d= 1m, and the propagation frequency f = 0.3 GHZ. The mesh used here corresponds to 12 points per wavelength. The figures (6) and (7) represent respectively the electric field and the magnetic field produced by the current. We can see the good quality of the approximate solutions compared to the exact ones.

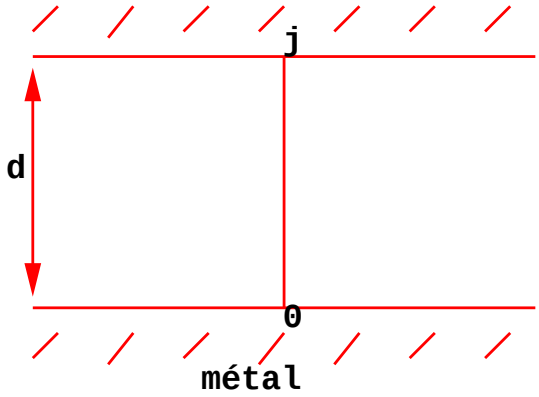

Figure 5: A sheet of current in a rectangular waveguide

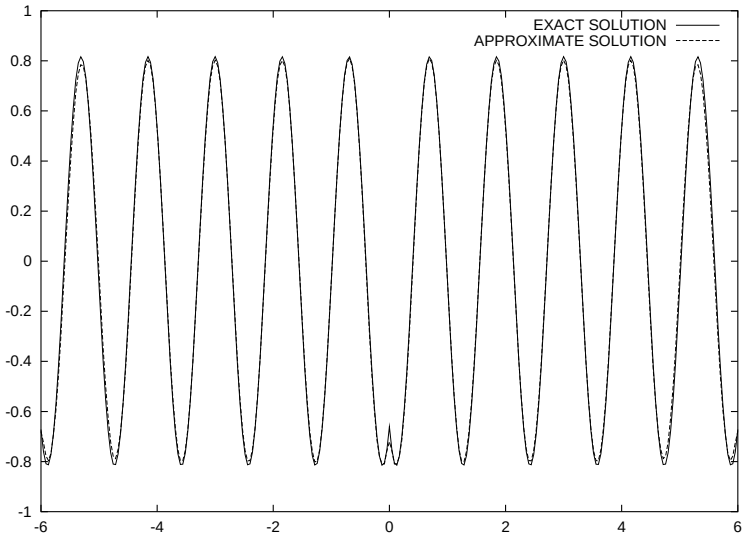

Figure 6: Section on y=$\frac{d}{2}$ of the electric wave E_z

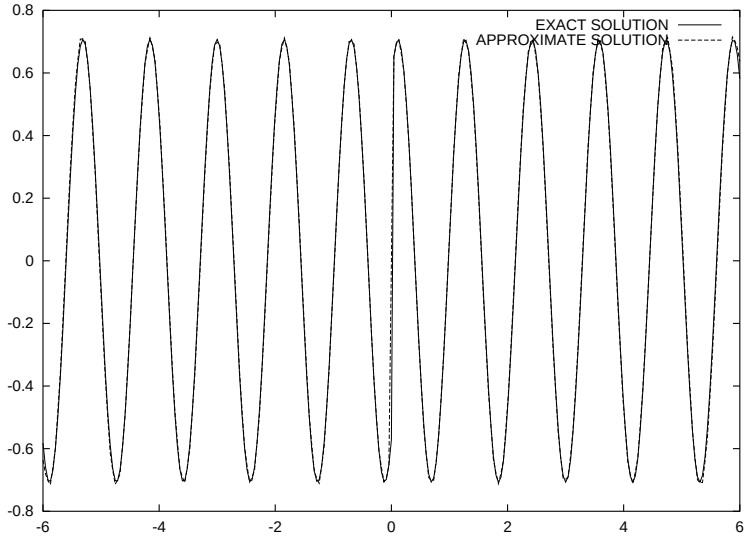

Figure 7: Section on y=$\frac{d}{2}$ of the magnetic wave H_y

3.3 Propagation of a pulse

We simulate the evolution of a pulse into a media composed of vacuum at right of $x = 0$ and a glass at the left ($\varepsilon = 4$, and $\mu = 1$). The mesh used in this experiment corresponds to ten points per wavelenght in the dielectric material. The approximate solution is compared to the exact one, and we can notice the good quality of the numerical solution (figure 8).

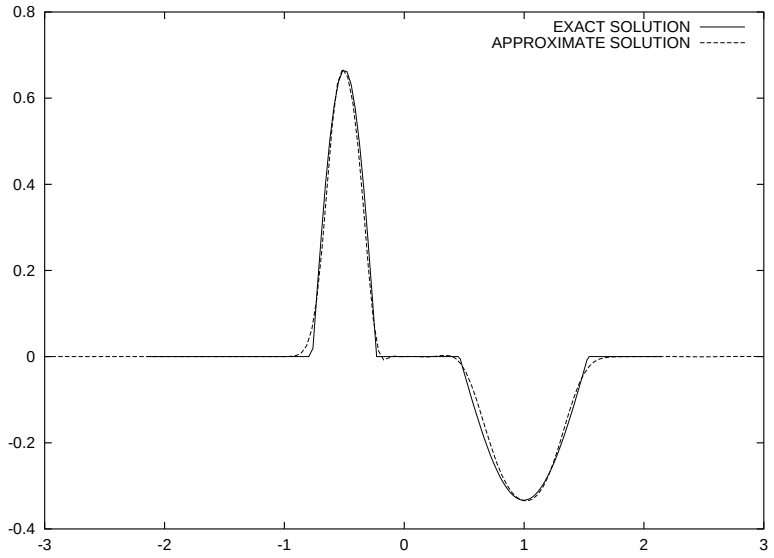

Figure 8: Propagation of a pulse into an heterogeneous media

3.4 Scattered wave across a dielectrical material

We propose here to simulate a scattering problem in an heterogeneous case. We illuminate a coated NACA0012 whoses mesh corresponds to 15 points per wavelenght (figure 9) by a monochromatic wave placed at right of the object. We assume a dielectric layer of thickness $\delta = 0.1\lambda$ (with $\varepsilon = 4$ and μ=1). The figure (10) represents the isolines of the scattered electric wave, and we can notice that the numerical solution doesn't present any oscillation at the interface between the different media.

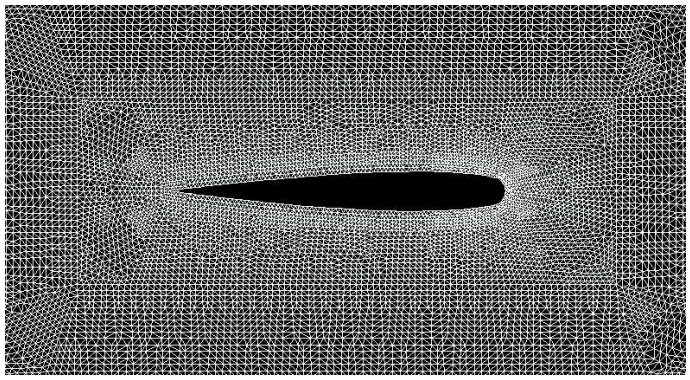

Figure 9: The NACA0012 mesh

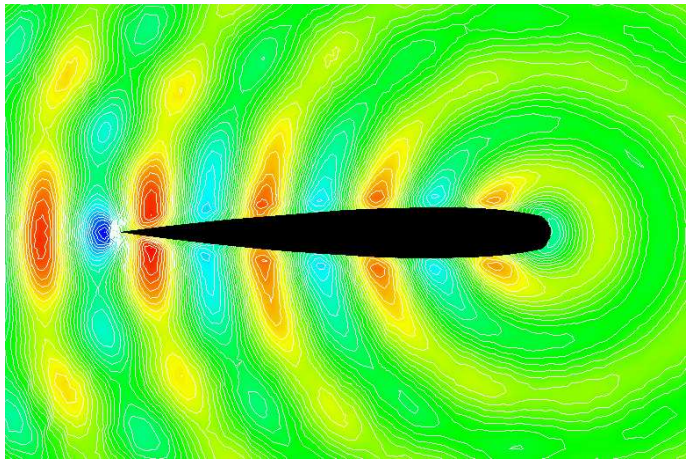

Figure 10: The scattered electric wave

3.5 Comparison with a MUSCL finite volume method

We propose to compare our method with a MUSCL finite volume method which is based on high upwind scheme in space, and a Runge-Kutta scheme in time with three steps. This scheme is third order accurate on structured grids. We consider a simple case, which represents the same experience as in the paragraph (3.1). We use the same mesh for the two methods (same number of degree of freedom). We can notice that the new finite volume method diffuse less than the MUSCL finite volume one (figure 11). The time of computation given by the new method is arround 23 seconds, and by the MUSCL method is arround 57 seconds. Thus, we can notice that the new method gives better CPU performance than the MUSCL finite volume one.

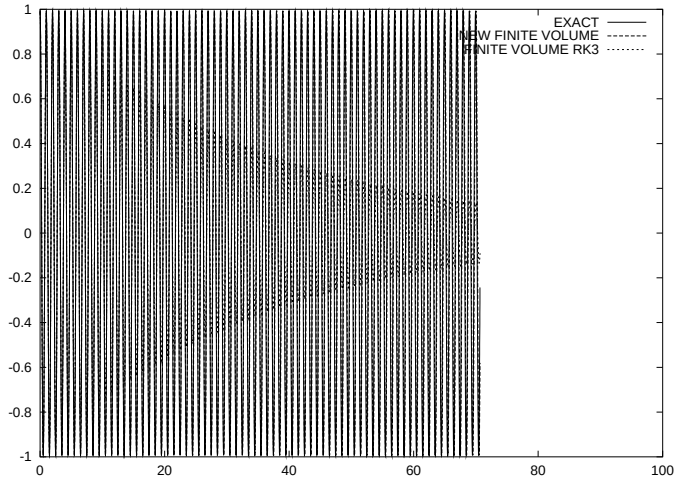

Figure 11: Comparison between two finite volume methods

4 Conclusion

We have presented in this paper a second order finite volume scheme to resolve the Maxwell equations. Theoretical analysis of the method was presented, and numerical experiments were investigated. This study shows that this technique of approximation is well appropriate to resolve the electromagnetic problems in a linear case, but not necessary homogeneous. The advantages of this method compared to the others finite volume methods are its simplicity implementation, and its flexibility to handle with complicated geometries since all the field vectors are lacated at the same points. We can also notice the numerical conservation of the energy. Owing to these propreties, it seems to be the most appropriate method to be combined with the finite difference method [9] in order to obtain a hybrid scheme for the Maxwell equations in complicated domains. An hybridation technique is in study.

5 Aknowledgement

I wish to thank Dr Loula Fezoui for her useful remarks and several advices. I would also like thank Dr Frederic Poupaud and Eric Duceau for their helpful.

References

[1] R.Carpentier, A.de la Bourdonnaye, B.Larrouturou, *On the derivation of the modified equation for the analysis of linear numerical methods*, Rapport de recherche CERMICS, no 26, (1994).

[2] J.P.Cioni, L.Fézoui, D.Issautier, *High-order upwind schemes for solving time-domain Maxwell equations*, La Recherche Aérospatiale, Vol 5, pp. 319-328, (1994).

[3] F.Hermeline, *Two coupled particle-finite volume methods using Delaunay-Voronoï meshes for the approximation of Vlasov-poisson and Vlasov-Maxwell equations*, J.Comp.Phy, Vol 106, pp 1 – 18, (1993).

[4] Niel.k.Madsen, Richard.W.Ziolkowsky, *A Three-Dimensional Modified Finite Volume Technique For Maxwell's Equations*, Electromagnetics, vol 10, no $1-2$, pp $147-161$, 1990.

[5] M.Remaki, L.Fézoui, F.Poupaud, *Un nouveau schéma de type volumes finis appliqué aux équations de Maxwell en milieu hétérogène*, rapport de recherche INRIA no 3351, janvier 1998.

[6] SHANKAR V. - HALL W.F. - MOHAMMADIAN A.H., *A time-domain differential solver for electromagnetic scattering problem, Proceeding on the IEEE*, Vol 77, pp. 709-721, No 5, (1989).

[7] A.Taflove, M.E.Brodwin, *Numerical Solution of Steady-State Electromagnetic Scattering problems Using the Time-Dependent maxwell's equations*, IEEETrans.Antenna Propagat, vol.MTT-23, no. 8, pp. 623-630, August (1975).

[8] R.F.Warming, F.Hyett, *The midified equation approach to the stability and accuracy analysis of finite-difference methods*, J.Comp.Phys., 14, (2), p.159, (1974).

[9] K.S.Yee, *Numerical solution of initial boundary value problem in isotropic media*, IEEE Trans.Antenna Propagat, vol.AP-14, no. 3, pp. 302-307, May (1966).

[10] K.S.Yee, J.S.Chen, *Conformal Finite Difference Time Domain and Finite Time Domain*, IEEE (1994).

[11] K.S.Yee, J.S.Chen, *Impedance Boundary Condition Simulation in the FDTD/FVTD Hybrid*, IEEE (1997).

Unité de recherche INRIA Sophia Antipolis
2004, route des Lucioles - B.P. 93 - 06902 Sophia Antipolis Cedex (France)

Unité de recherche INRIA Lorraine : Technopôle de Nancy-Brabois - Campus scientifique
615, rue du Jardin Botanique - B.P. 101 - 54602 Villers lès Nancy Cedex (France)
Unité de recherche INRIA Rennes : IRISA, Campus universitaire de Beaulieu - 35042 Rennes Cedex (France)
Unité de recherche INRIA Rhône-Alpes : 655, avenue de l'Europe - 38330 Montbonnot St Martin (France)
Unité de recherche INRIA Rocquencourt : Domaine de Voluceau - Rocquencourt - B.P. 105 - 78153 Le Chesnay Cedex (France)

Éditeur
INRIA - Domaine de Voluceau - Rocquencourt, B.P. 105 - 78153 Le Chesnay Cedex (France)
http://www.inria.fr
ISSN 0249-6399